DOI: http://doi.org/10.25130/tjes.32.2.20

IRAQI Academic Scientific Journals

ISSN: 1813-162X (Print); 2312-7589 (Online)

Tikrit Journal of Engineering Sciences

available online at: http://www.tj-es.com

TJES Tikrit Journal of Engineering Sciences

Performance Analysis of Optical Wireless Channel Based on Beamforming Techniques Using Advanced Modulation Schemes

Lwaa Faisal Abdulameer *[a], **Adil Fadhil Mushatet** [a], **Tania Tariq Salim** [b]

[a] Department of Information and Communication Engineering, Al-Khwarizmi College of Engineering, Baghdad University, Baghdad, Iraq.

[b] Department of Electrical Engineering Technologies, Electrical Engineering Technical College, Middle Technical University, Baghdad, Iraq.

Keywords:

Beamforming; GFDM; OFDM; OWC; Spectral efficiency.

Highlights:

- *The beamforming technique improved the spectral efficiency for various modulation formats.*
- *Optical-GFDM assisted beamforming function performed better in terms of bandwidth and power efficiency than the other modulation formats.*

ARTICLE INFO

Article history:

Received	21 July 2023
Received in revised form	07 Oct. 2023
Accepted	08 June 2024
Final Proofreading	01 Dec. 2024
Available online	31 May 2025

Citation: Abdulameer LF, Mushatet AF, Salim TT. **Performance Analysis of Optical Wireless Channel Based on Beamforming Techniques Using Advanced Modulation Schemes**. *Tikrit Journal of Engineering Sciences* 2025; **32**(2): 1397. http://doi.org/10.25130/tjes.32.2.20

*Corresponding author:

Lwaa Faisal Abdulameer

Department of Information and Communication Engineering, Al-Khwarizmi College of Engineering, Baghdad University, Baghdad, Iraq.

Abstract: The need for a very high data rate in the next-generation wireless network is growing, and optical wireless communication has become one of the best options for addressing this important problem. The optical system endures power and bandwidth losses due to channel turbulence, particularly in the extreme channel conditions found in outdoor locations. However, suitable advanced optical modulation schemes categorized according to the appropriateness of power efficiency and suitability of bandwidth-efficient systems are used to ensure transmission reliability. In this study, orthogonal frequency-division multiplexing, generalized frequency-division multiplexing, and L-pulse position modulation are used. Utilizing the cutting-edge GFDM-Beamforming technology for the optical wireless channel was to increase the signal to noise ratio and enhance the bit error rate across the board. Gamma-Gamma distribution has been used to compute the bit error rate and spectral efficiency. An arbitrary number of light-emitting diodes and photo-detectors are used at the sources and detectors. The findings demonstrated that the optical generalized frequency-division multiplexing performs better than other modulation schemes in terms of power and bandwidth requirements, with a high peak-to-average-power-ratio, which is the primary drawback in orthogonal frequency-division multiplexing mitigated by the beamforming function.

تقييم الأداء لقناة ضوئية لاسلكية معتمدة على تقنيات تكوين الشعاع بأستخدام مخططات تضمين متقدمة

لواء فيصل عبد الامير ١، عادل فاضل مشتت ١، تانيا طارق سالم ٢
١ قسم هندسة المعلومات والاتصالات/ كلية هندسة الخوارزمي/ جامعة بغداد/ بغداد - العراق.
٢ قسم تقنيات الهندسة الكهربائية/ الكلية التقنية للهندسة الكهربائية/ الجامعة التقنية الوسطى/ بغداد - العراق.

الخلاصة
تتزايد الحاجة إلى معدل بيانات مرتفع للغاية في الجيل القادم من الشبكات اللاسلكية، وأصبح الاتصال اللاسلكي البصري أحد أفضل الخيارات لمعالجة هذه المشكلة المهمة. يتحمل النظام البصري خسائر في الطاقة وعرض النطاق الترددي نتيجة لاضطراب القناة، لا سيما في ظروف القناة القاسية الموجودة في المواقع الخارجية. ومع ذلك، يتم استخدام مخططات تعديل بصري متقدمة مناسبة يتم تصنيفها وفقًا لمدى ملاءمة كفاءة الطاقة ومدى ملاءمة الأنظمة الفعالة لعرض النطاق الترددي لضمان موثوقية الإرسال .في هذه الدراسة، تم استخدام تعدد الإرسال المتعامد بتقسيم التردد، تعدد الإرسال بتقسيم التردد المعمم وتعديل موضع النبضة. أضافة الى ذلك تم الاستفادة من تقنية تكوين الشعاع باستخدام تعدد الإرسال بتقسيم التردد المعمم المتطورة للقناة اللاسلكية الضوئية لزيادة نسبة الإشارة إلى الضوضاء وتعزيز معدل الخطأ في البت. توزيع كاما-كاما أستخدم في هذه الدراسة لحساب معدل الخطأ في البت وكفاءة الطيف الترددي بوجود عدد من الثنائيات الباعثة للضوء عند الأرسال والكواشف الضوئية عند الأستقبال. النتائج المستحصلة بينت على ان تعدد الإرسال بتقسيم التردد المعمم الضوئي يؤدي أداءً أفضل مقارنة مع طرق التضمين الأخرى من حيث متطلبات القدرة وعرض النطاق الترددي مع قيمة عالية لنسبة الذروة إلى متوسط قدرة والتي تعتبر واحدة من العيوب الأساسية لتقنية تعدد الإرسال المتعامد بتقسيم التردد والذي تم معالجته عن طريق تقنية تكوين الشعاع.

الكلمات الدالة: تكوين الشعاع، تعدد الإرسال بتقسيم التردد المعمم، تعدد الإرسال المتعامد بتقسيم التردد الضوئي، قناة ضوئية لاسلكية، الطيف الترددي.

1.INTRODUCTION

Recently, high-dense networks and lower data rates have resulted from the rising demands for high data rates brought on by a significant increase in traffic in small cells [1, 2]. Optical wireless communication (OWC) is a new and alternative technology that addresses the network access bottleneck by ensuring the efficient transmission availability between transceivers and overcoming the limitations of radio frequencies that suffer from low data rates, especially at the last mile connection [2]. OWC's license-free, enormous bandwidth potential, more than 10 Gb/s data rate, easy implementation, and superior security made it a crucial supplementary alternative to RF [3]. Despite these potential benefits, atmospheric turbulence brought on by meteorological influences causes fluctuations in the OWC link's phase and magnitude, resulting in a deep fade. However, as air turbulence's effect increases from weak to strong, the OWC performance suffers significantly [4]. Choosing a modulation scheme appropriate for the system is crucial since it affects its power and bandwidth efficiency [5]. While pulse position modulation (PPM) can achieve high-power efficiency at the expense of spectral efficiency due to an increase in the bandwidth requirement. Some modulation schemes, such as multi-Level-pulse amplitude modulation (L-PAM), improve spectral efficiency by increasing the pulsed bandwidth laser, however, at the cost of less power. Due to its simplicity and ability to provide acceptable power requirements, On-Off Keying (OOK) is the technique most frequently employed in OWC; however, it is particularly susceptible to air turbulence. Due to its capacity to counter ISI, OFDM is most useful with interferer free space channels [5-7]. A viable choice for applying OWC is the Generalized Frequency Division Multiplexing (GFDM) approach, as it is designed to address the high peak-to-average power ratio (PAPR) issue associated with OFDM by incorporating filtering and pulse shaping, good spectral efficiency, and the capacity to reduce channel interference [8]. In terms of lowering PAPR and out-of-band radiation, GFDM performs better than OFDM. Establishing an accurate line of sight link between sources and detectors and controlling the beam divergence angle, particularly for long-range (>1Km) systems to provide enough energy at the receiver side, are the key challenges in OWC. However, how much energy will reach the receiver determines the OWC signal's availability and stability [9]. A promising approach to ensuring dependable transmission between two OWC terminals is beamforming [4]. The Beamforming function efficiently controls the signal strength and the beam divergence angle [10]. However, in the presence of severe OWC channel characteristics such as turbulence and scintillation, beamformers have limits to noise reduction [11-14]. Different methods have been researched for observing OWC system performance. Optical multiple-input multiple-output (MIMO) links have been introduced in [15] to enhance system performance overall [15, 16]. According to [17], a simulation approach has been put forth to model the performance of M-ary quadrature amplitude modulation (M-QAM) with spatial diversity to offer data on outage probability and bit error rate (BER) while accounting for OWC system disturbances. According to BER, various channel restrictions, and turbulences, the performance of a single-input, multiple-output (SIMO) OWC system based on the M-ary phase shift keying (M-PSK) modulation format was examined in [18]. To enhance the OWC systems, a Space Shift Keying (SSK) method has been introduced in [19]. The error probability of OWC systems based on subcarrier intensity modulation has been examined in [20] utilizing lognormal connections. A spatially diverse OWC system over Gamma-Gamma was studied in [21]. It has been shown that transmit diversity and the PPM modulation method enhanced the OWC-based optical spatial modulation's performance [22-24]. In the present study, advanced modulation techniques, including L-PPM, OFDM, and GFDM, have been combined with the beamforming function to increase the signal-to-noise ratio and, as a result, deliver high-efficiency signal intensity at the receiver by lowering the beam divergence angle. To the best of the authors' knowledge, the chosen approach, which explored the potential of GFDM to significantly improve both the spectral and power efficiency utilizing the beamforming technique, has yet to be considered.

2.THEORETICAL ANALYSIS

2.1.Beamforming PPM

The L-PPM signal, s (t), consists of a pulse with a slot duration (T_s), and L denotes the number of time slots, i.e., L= 2^Q (Q > 0). As is common practice in PPM, data is encoded in a pulse whose position is determined to correspond to Q-bit input data. The transmitted pulse, however, is provided by:

$$s(t)_{PPM}\begin{cases} 1\ for\ t \in (q-1)T_{s,PPM}, qT_{s,PPM} \\ 0\ , otherwise \end{cases} \quad (1)$$

where $T_{s,PPM} = T_b Q$, T_b is the bit duration, and $q \in \{1,2,\dots,L\}$.

As a result, each Laser Diode (LD)'s transmitted bits sequence modulation is indicated by:

$$S_{owc}(\mathbf{t}) = \mathrm{L}\, P_{avg} \sum_{k=0}^{L-1} S_k \quad (2)$$

where S_k is the PPM bit sequence $\{S_0, S_1, \dots, S_{L-1}\}$, and P_{avg} is the average transmitted power. The pulse shaping is disregarded in this notation. Considering that a driving circuit converts the modulated voltage signal into a pleasant current signal given to the LD. The signal received at the photo-detectors PDs through additive white Gaussian noise (AWGN), affected by air turbulence for the proposed system with M sources and N PDs., can be described as:

$$y_n = R \sum_{m=0}^{M-1} H_{mn} S_{owc(m)} + V_n, n = 0, 2 \dots . N-1 \quad (3)$$

where R is the detector responsiveness, and $S_{owc(m)}$ is the transmitted signal from the m^{th} source. V_n is AWGN with variance σ_v^2, and H_{mn} is the irradiance from the m^{th} source and the n^{th} detector. The irradiance can be stated in OWC as:

$$H_{mn} = H_{emn} H_{smn} H_{pmn} \quad (4)$$

where H_{emn} stands for the attenuation brought on by path loss and beam extinction. H_{smn} represents the effects of scintillation. H_{pmn} stands for the geometric spread and mispointing error. The received signal vector from each aperture is represented by:

$$\overline{y_n} = R \sum_{i=0}^{I-1} \sum_{m=0}^{M-1} H_{mn}(i)\ \bar{S}_{OWC,m} + \overline{V_n}$$
$$i, n \in \{0, 1, 2, \dots . I-1\} \quad (5)$$

where I is the directed beam intensity from the sources (LDs). Each y and V in Eq. (5) has dimensions of (n×1), and H is a matrix with dimensions of (n×m). So:

$$\overline{y_0} = R \sum_{i=0}^{I-1} \sum_{m=0}^{M-1} H_{mn}(i)\ \bar{S}_{OWC,m} + \overline{V_0} \quad (6)$$

$$\overline{y_1} = R \sum_{i=0}^{I-1} \sum_{m=0}^{M-1} H_{mn}(i)\ \bar{S}_{OWC,m} + \overline{V_1} \quad (7)$$

$$\overline{y_{N-1}} = R \sum_{i=0}^{I-1} \sum_{m=0}^{M-1} H_{mn}(i)\ \bar{S}_{OWC,m} + \overline{V}_{N-1} \quad (8)$$

One alternative for these equations is:

$$\begin{bmatrix} y_0 \\ y_1 \\ \cdot \\ y_{N-1} \end{bmatrix} = R \sum_{i=0}^{I-1} \sum_{m=0}^{M-1} \begin{bmatrix} H_{11} & \cdot & \cdot\ H_{0,m-1} \\ H_{21} & \cdot & \cdot\ H_{2,m-1} \\ H_{N-1,1} & \cdot & \cdot H_{N-1,m-1} \end{bmatrix} \bar{S}_{OWC,m} + \begin{bmatrix} V_1 \\ V_2 \\ \cdot \\ V_{N-1} \end{bmatrix} \quad (9)$$

To estimate the derived beam, all the received beams must be merged at the required destination. Consequently, the combined signal can be written as:

$$B_0^* y_0 + B_1^* y_1 + \dots . . + B_{N-1}^* y_{N-1} \quad (10)$$

The equations above are written as:

$$[B_0^* \quad B_1^* \quad \cdot \quad \cdot \quad B_{N-1}^*] \begin{bmatrix} y_0 \\ y_1 \\ \cdot \\ \cdot \\ y_{N-1} \end{bmatrix} = B^{-H}\, \bar{y} \quad (11)$$

where B stands for the beamformer, and the up-script H denotes the matrix's Hermitian. Remember that in wireless communications,

$$\bar{y} = H\bar{S} + \bar{V} \quad (12)$$

$$\bar{y} = R(\bar{B}^H H_{mn} . \bar{S}_{OWC,m} + \bar{B}^H \bar{V}) \quad (13)$$

The desired beam's signal components are represented in the first half of the above equation, while the desired beam's noise components are represented in the second. The signal power of the desired beam can be computed as:

$$\textbf{signal power} = R\, |\bar{B}^H H_{mn}|^2 \cdot P_d \cdot L \quad (14)$$

where P_d is the intended signal's power, calculated as:

$$E\{S_i S_j\} = E \begin{bmatrix} S_{11} & \cdots & S_{1j} \\ S_{21} & \ddots & S_{2j} \\ \vdots & \cdots & \vdots \\ S_{i1} & & S_{ij} \end{bmatrix} = \begin{bmatrix} P_d & 0 & 0 \\ 0 & P_d & 0 \\ 0 & 0 & P_d \end{bmatrix} = P_d I \quad (15)$$

$E\{S_i S_j\} = P_d$ when i=j and $E\{S_i S_j\} = 0$ when i≠j

Now, the effective noise at the beamformer's output may be calculated from:

$$E\{|\bar{B}^H \bar{V}|^2\} = E\{(\bar{B}^H \bar{V})(\bar{B}^H \bar{V})^*\} \quad (16)$$

$$E(\overline{B}^H\overline{V}\ \overline{V}\ \overline{B}) = \overline{B}^H E(\overline{V}\ \overline{V})\overline{B} \qquad (17)$$

$$E(\overline{V}\overline{V}^H) = E\begin{bmatrix} |V_{11}|^2 & V_1V_2^* \cdots V_1V_{N-1}^* \\ V_2V_1^* & |V_{22}|^2 \cdots V_2V_{N-1}^* \\ \vdots & \vdots \\ V_{N-1}V_2^* & \cdots |V_{N-1}|^2 \end{bmatrix} = \sigma_V^2 I \qquad (18)$$

where $E\{V_iV_j\}= \sigma_V^2$ when i = j and 0 when i ≠ j. Hence,

$$\textbf{Noise power} = \sigma_V^2\ ||\overline{B}\ ||^2 \qquad (19)$$

where || || denotes the norm.

After that, the maximum signal-to-noise ratio can be calculated as:

$$SNR_{max} = \frac{R\,|\,\overline{B}^H H_{mn}\ |^2 .\ P_d.L}{\sigma_V^2\ ||\overline{B}\ ||^2} \qquad (20)$$

The computational BER for L-PPM in the example being studied can be calculated from the determined SNR_{max} above, as follows:

$$BER(H_{mn}) = 0.5 \times erfc(\sqrt{SNR_{max}}) \qquad (21)$$

$$BER(H_{mn}) = 0.5 \times erfc\left(\sqrt{\frac{R\,|\,\overline{B}^H H_{mn}\ |^2 .\ P_d.L}{\sigma_V^2\ ||\overline{B}\ ||^2}}\right) \qquad (22)$$

A probability density function is utilized to represent the channel in the form of Meijer's G function represented in Eq. (20) and calculate the average BER across strong atmospheric turbulence, as follows:

$$f_{Hmn}(hmn) = \frac{\alpha_{mn}\beta_{mn}\varepsilon_{mn}^2}{A_{omn}H_{lmn}\Gamma(\alpha_{mn})\Gamma(\beta_{mn})} \times C_{1,3}^{3,0}\left[\frac{\alpha_{mn}\beta_{mn}H_{mn}}{A_{omn}H_{lmn}}\right]_{-1+\varepsilon_{mn}^2,\alpha_{mn}^{-1},\beta_{mn}^{-1}}^{\varepsilon_{mn}^2} \qquad (23)$$

where α and β represent the effective number of large- and small-scale turbulent eddies, Γ(.) represents the Gamma function, A_{omn} represents the highest percentage of the gathered power in the receiving lens, and $\varepsilon_{mn}^2(= a\sigma_p)$ represents the ratio between the deviation of the mispointing and the beam radius. The average error probability is thus represented as:

$$p_e = \int_0^\infty BER(H_{mn}) f_{Hmn} dH \qquad (24)$$

Hence,

$$p_e = \frac{\alpha_{mn}\beta_{mn}\varepsilon_{mn}^2}{A_{omn}H_{lmn}\Gamma(\alpha_{mn})\Gamma(\beta_{mn})} \times \int_0^\infty 0.5 \times \text{erfc}\left(\sqrt{\frac{R\,|\,\overline{B}^H H_{mn}\ |^2 .\ P_d.L}{\sigma_V^2\ ||\overline{B}\ ||^2}}\right) \times C_{1,3}^{3,0}\left[\frac{\alpha_{mn}\beta_{mn}H_{mn}}{A_{omn}H_{lmn}}\right]_{-1+\varepsilon_{mn}^2,\alpha_{mn}^{-1},\beta_{mn}^{-1}}^{\varepsilon_{mn}^2} . dH \qquad (25)$$

2.2. Beamforming OFDM

A block of QAM symbols is $d = [d_0\ d_1 \ldots d_{D-1}]$, and symbol time $T_s = \frac{C}{B_W}$ allows the complete bandwidth (B_W) to be divided into C sub-carriers. The output OFDM signal, however, is represented as,

$$S_{OFDM,m} = \sum_{i=0}^{C-1} d_i e^{\frac{j2\pi ic}{C}}, c \in \{0, 1, \ldots C-1\} \qquad (26)$$

where, $E\{d_id_i^*\} = \sigma_d^2\ if\ i = j$ and $E\{d_id_i^*\} = 0$ if i ≠ j. Applying cyclic prefix (CP), then,

$$S_{cp,m} = \sum_{i=0}^{C-1} d_i\ e^{\frac{j2\pi ic}{C}}, S_{cp,m} = [s(c + Lcp - 1, s(c-1; c] \qquad (27)$$

To make the OFDM signal comfortable for the LDs inputs, the signal $S_{OFDM,m}$ can be applied to the driven circuit. Hence,

$$I_m = 2P_{avg} \sum i_{cp}\ e^{\frac{j2\pi ic}{C}} \qquad (28)$$

Eq. (2) denotes the signal produced by the m^{th} optical source. The multipath (direct and non-direct) between M sources and N detectors is related to the channel matrix H_{mn}, as was discussed in the previous section in Eq. (4). Consequently, the signal obtained at the PDS using AWGN is impacted by:

$$y_{OFDM} = R\sum_{m=0}^{M-1} H_{mn} I_i\ W_N + \overline{V_n} \qquad (29)$$

where W_N is the N point inverse-fast Fourier transform (IFFT).

Now, let H_mn be a circulant matrix and can be factorized as,

$H_{mn} = WFW^H$,

Where

$$F = \sqrt{N} \times \begin{bmatrix} W_N^H|H_{11}|^2 & 0 & 0 \\ 0 & W_N^H|H_{22}|^2 & 0 \\ 0 & 0 & 0 \\ 0 & 0 & W_N^H|H_{M-1,1N-}|^2 \end{bmatrix} = \begin{bmatrix} W_N^H\sigma_1^2 & 0 & 0 \\ 0 & W_N^H\sigma_2^2 & 0 \\ 0 & 0 & W_N^H\sigma_{M-1}^2 \end{bmatrix} \qquad (30)$$

where σ_i is the gain of the channel. Thus, the received signal following the removal of CP is provided by,

$$\overline{y_n} = R\sum_{i=0}^{N-1} I_i(W_N F W_N^H \sigma_i + \overline{V_n}) = R\sum_{i=0}^{M-1} W_N F I_i \sigma_i + \overline{V_n} \qquad (31)$$

The N-point FFT is computed as:

$$\overline{Z_n} = W_N^H y_n = R\sum_{i=0}^{N-1} F I_i \sigma_i + \overline{V_n} \qquad (32)$$

Applying beamforming to the above formula to increase SNR and calculate the ideal beam. As a result, the total received signals are given as:

$$B_0^* Z_{0+} B_1^* Z_1 + \cdots \ldots + B_{N-1}^* Z_{N-1} = \overline{B}^H \overline{Z_H} \qquad (33)$$

$$\overline{Z} = R\overline{B}^H F \sum_{i=0}^{N-1} I_i \sigma_i + \overline{B}^H\ \overline{V_n}\ W^H \qquad (34)$$

The intended beam's signal power is calculated as:

$$\textbf{Signal power} = |B^H F\ |^2 \sum_{i=0}^{M-1} \sigma_i\, P_d . 2P_{avg} R \qquad (35)$$

The effective noise at the beamformer's output is calculated as:

$$E\{\overline{B}^H\ \overline{V}_n W^H\} = E\{(\overline{B}^H \overline{V} W^H)(\overline{B}^H \overline{V} W^H)\} = \overline{B}^H B\ W^H W E\{\overline{V}\ V^H\} = \sigma_V^2\ ||B\ ||^2 ||W\ ||^2 \qquad (36)$$

Hence,

$$SNR_{max} = \frac{2P_{avg}R\,|\,\bar{B}^H\ F\ |^2.\ P_d.\sum_0^{M-1}\sigma_i}{\sigma_V^2\,||B\,||^2||W\,||^2} \quad (37)$$

Following that, the suggested beamforming OFDM system's average BER is calculated as follows:

$$BER(H_{mn}) = 0.5 \times erfc(\sqrt{SNR_{max}}) \quad (38)$$

In section (2.1), Eq. (23) states that under the same circumstances, the likelihood of error is represented as:

$$p_e = \frac{\alpha_{mn}\beta_{mn}\varepsilon_{mn}^2}{A_{omn}H_{lmn}\,\Gamma(\alpha_{mn})\Gamma(\beta_{mn})} * \int_0^{\infty} 0.5 \times \mathrm{erfc}\left(\sqrt{\frac{2P_{avg}R\,|\,\bar{B}^H\ F\ |^2.\ P_d.\sum_0^{m-1}\sigma_{i_i}}{\sigma_V^2\,||B\,||^2||W\,||^2}}\right) \times G_{1,3}^{3,0}\left[\frac{\alpha_{mn}\beta_{mn}H_{mn}}{A_{omn}H_{lmn}}\right]_{-1+\varepsilon_{mn}^2,\alpha_{mn}^{-1},\beta_{mn}^{-1}}^{\varepsilon_{mn}^2} . dH \quad (39)$$

2.3. Beamforming GFDM

In general, consider a QAM. A block of symbols is organized as follows:

$$d = [d_0\ d_1 \ldots d_{TC-1}]^T \quad (40)$$

where the expected value of $d_i d_j = \sigma_d^2$ when $i = j$, and the expected value of $d_i d_j = 0$ when $i \neq j$. In contrast to OFDM, GFDM forms the transmitted signal as a block of time slots or two-dimensional symbols, i.e., T time slots multiplied by C subcarriers. Therefore, C subcarriers are transmitted throughout each time slot. To represent the data of dimension TC×1,

$$d = [d_{0,0} \ldots d_{t,c} \ldots d_{T-1}d_{C-1}] \quad (41)$$

are considered at transmitter, where $t = 0,1,\ldots T-1$, and $c(=0,1,\ldots C-1)$ represents time slot index and subcarrier index respectively. The driven circuit converts the modulated data into a signal convenient for the LD source using a GFDM Modulator. A pulse shape $g(a)$ is considered as an impulse response for data d in the dimensions $MN \times 1$; then,

$$X_{t,c}(n) = \sum_{r=0}^{MN-1} d_{t,c}\ g(n-r) = d_{t,c}.\,g(n-mN) \quad (42)$$

Using IFFT, the data is separated into C subcarrier frequencies, i.e.,

$$X_{t,c}(n) = \sum_{r=0}^{MN-1} d_{t,c}\ g(n-r).\,e^{\frac{j2\pi nc}{C}} \quad (43)$$

The GFDM signal is expressed as,

$$X_{t,c}(n) = \sum_{l=0}^{MN-1} a_l^N(n) d_l^N \quad (44)$$

where $X_{t,c}(n) = d_{t,c}\ a_{t,c}(n)$. However, the output samples of the GFDM is:

$$\bar{X} = \sum_{i=0}^{MN-1} a_l^{-c}\ d_l^c \quad (45)$$

where,

$$\bar{X} = [X(0), X(1), \ldots X(mN-1)]^T \quad (46)$$

$a_l^c = [a_l^c(0) \quad a_l^c(1) \ldots\ a_l^c(mn-1)\,] = \bar{A}$

where a_l^c is the modulation index, and $\overline{d^C}(= [d_0\ d_1, \ldots d_{MN-1}]^T)$ is the date vector. A CP is added to the GFDM modulated signal and applied to the driven circuit to prevent Inter Block Interference (IBI), i.e.,

$$\overline{I_{CP}}(n) = 2P_{avg}[I(MN - C_{cp} + 1{:}\,Mn); \bar{I}] \quad (47)$$

The signal received at the PDs is impacted by atmospheric turbulence, as seen in the analysis above, and is stated as:

$$\overline{y_{cp}} = R\sum_i H_{mn} I_{CP(i)} + \overline{V_n} \quad (48)$$

C_{CP} and $L-1$ are samples that will be taken out of $\overline{y_{cp}}$ at the receiver, and the signal is then transformed into,

$$\bar{y} = R\sum_i Hmn\ A\bar{\imath}\ d\bar{\imath} + \overline{V_n} \quad (49)$$

A beamformer is used to integrate all received signals at a particular aperture and estimate the best-desired beam. Then,

$$B_0^* y_0 + B_1^* y_1 + \cdots B_{MN-1}^* y_{MN-1} = \bar{B}^H \bar{y} \quad (50)$$

Hence,

$$\bar{y} = R\sum_i \bar{B}^H\, H_{mn}\, A_i\, di + \bar{B}^H n \quad (51)$$

Then, the signal power is given by:

$$\textbf{Signal power} = R\sum_i \bar{B}^H\ \ H_{mn}\, A_i|^2 P_d \quad (52)$$

The effective noise of the output of the beamformer can be computed as:

$$E\{\bar{B}^H \bar{V}_n^H \bar{B}\ \bar{V}_n\} = \bar{B}^H BE\{\bar{V}_n^H \bar{V}_n\} = \sigma_V^2\ \overline{||B||}^2 \quad (53)$$

Then, the maximized SNR using the GFDM modulator is:

$$SNR_{max} = \frac{R\sum_i \bar{B}^H\ \ H_{mn}\,\overline{A_i}|^2 P_d}{\sigma_V^2\ \overline{||B||}^2} \quad (54)$$

Consequently, the probability of error in this instance is represented by:

$$p_{e,GFDM} = \frac{\alpha_{mn}\beta_{mn}\varepsilon_{mn}^2}{A_{omn}H_{lmn}\Gamma(\alpha_{mn})\Gamma(B_{mn})} \times \int_0^{\infty} 0.5 \times \mathrm{erfc}\left(\sqrt{\frac{R\,|\,\sum_i \bar{B}^H\, H_{mn}\overline{A_i}\ |^2.\ P_d.}{\sigma_V^2\,||\bar{B}\,||^2}}\right) \times G_{1,3}^{3,0}\left[\frac{\alpha_{mn}\beta_{mn}H_{mn}}{A_{omn}H_{lmn}}\right]_{-1+\varepsilon_{mn}^2,\alpha_{mn}^{-1},B_{mn}^{-1}}^{\varepsilon_{mn}^2} .\,dH \quad (55)$$

3. RESULTS AND DISCUSSION

The simulation results used to confirm the effectiveness of various scenarios, including various sophisticated modulation techniques and beamforming, are shown in this section. Plots have been drawn showing the performance in terms of BER. Analysis has been done on the effects of scintillation and turbulence on various modulation schemes over the Gamma-Gamma channel model. C equaled 128 subcarriers in total. The 16 QAM signaling has been chosen. The values of α and β used for the scintillation effect were 4.19 and 2.27, respectively. As OOK is the most frequent modulation technique employed in OWC, it will be considered a reference technique to evaluate the performance of the more advanced modulation formats. Figure 1 shows the bandwidth and power requirements for OOK, L-PPM, optical OFDM, and optical GFDM. The bandwidth requirements are related to the achievable data rate R_b, and according to computed maximized SNR for each type of the modulation formats, the total channel capacity for M sources and N detectors is given as:

$$R_b \sum_{i=1}^{M} log_2 (1 + SNR)$$

which represents the sum of individual capacities of M information streams. The trade-off between optical power and bandwidth requirements is shown in Figure 1. The power requirements for the conventional modulation method used in OWC and OOK decreased with the duty cycle while increasing bandwidth in response. The bandwidth requirements for L-PPM continuously increased with the number of time slots (L). Optical-GFDM performed better in terms of bandwidth efficiency than optical-OFDM due to the structure of the transmitted signal for the GFDM scheme, formed as a block-time slot (two-dimensional), with successive increases in the bandwidth requirements. However, the optical power requirements increased insignificantly. Due to these findings, optical-GFDM is a good choice for the future generation of wireless communications, which must have a large bandwidth and use little power.

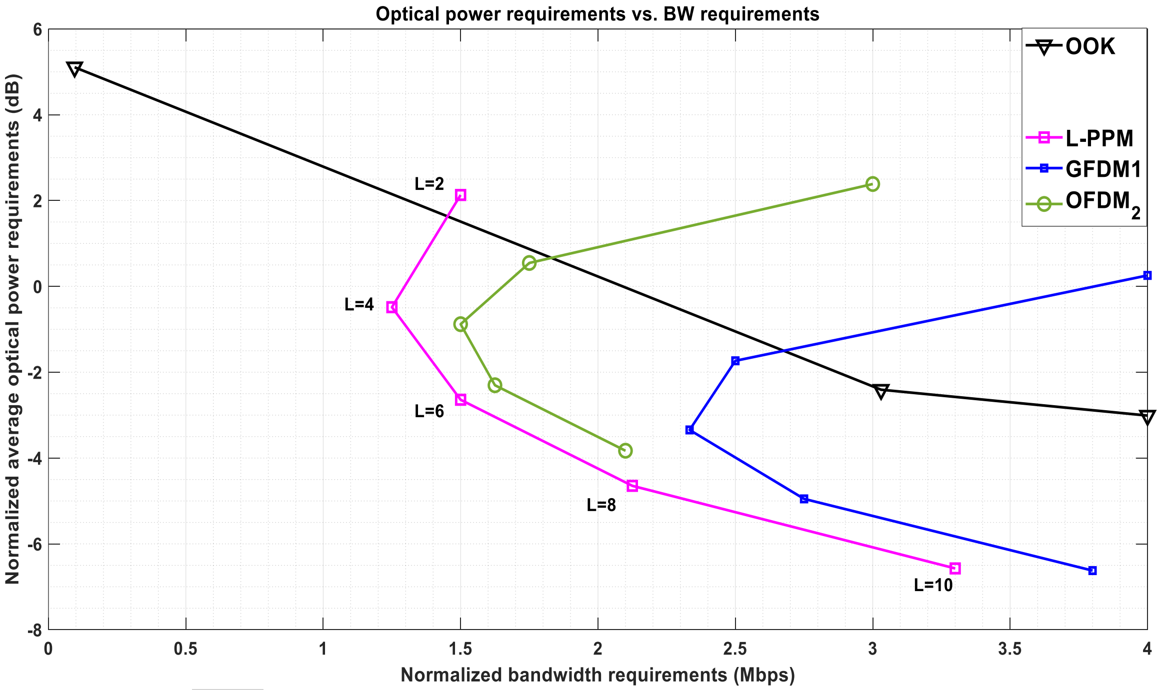

Fig. 1 Optical Power Requirements vs. Bandwidth Requirements.

With the aid of the beamforming function, which increases optical tracking effectiveness and system SNR, simulation evidence on advanced modulation methods was considered in this investigation. The likelihood of error for the OOK, L-PPM, optical-OFDM, and optical-GFDM is plotted versus the SNR in Fig. 2, showing a medium scintillation effect BER with a refractive index structure constant of 10−15. When BER was 10-5, optical-OFDM performed better than other schemes because it only needs around 12 dB SNR, whereas regular OOK needs about 16 dB SNR. Due to the nature of the transmitted symbols in GFDM, emitted in a block-time manner and causing some synchronization issues at the receiver side, optical-GFDM performed better at high SNR than optical-OFDM. Figure 3 shows the performance evaluation of several optical modulation techniques using the beamforming function. As illustrated, the optical-GFDM has higher spectral efficiency than the optical-OFDM over OWC. However, at least -10 dB SNR is required, whereas optical-OFDM requires -8 dB to obtain a spectral efficiency of 10 (bit/s/Hz). The literature claims that OFDM's main shortcoming is a high PAPR, even though its spectral efficiency is good. Thus, strong evidence of the GFDM-aided beamforming function was discovered when the present findings showed that GFDM had lower power requirements than the other schemes investigated and performed better in terms of spectral efficiency, making it a promising candidate for the next wireless technology.

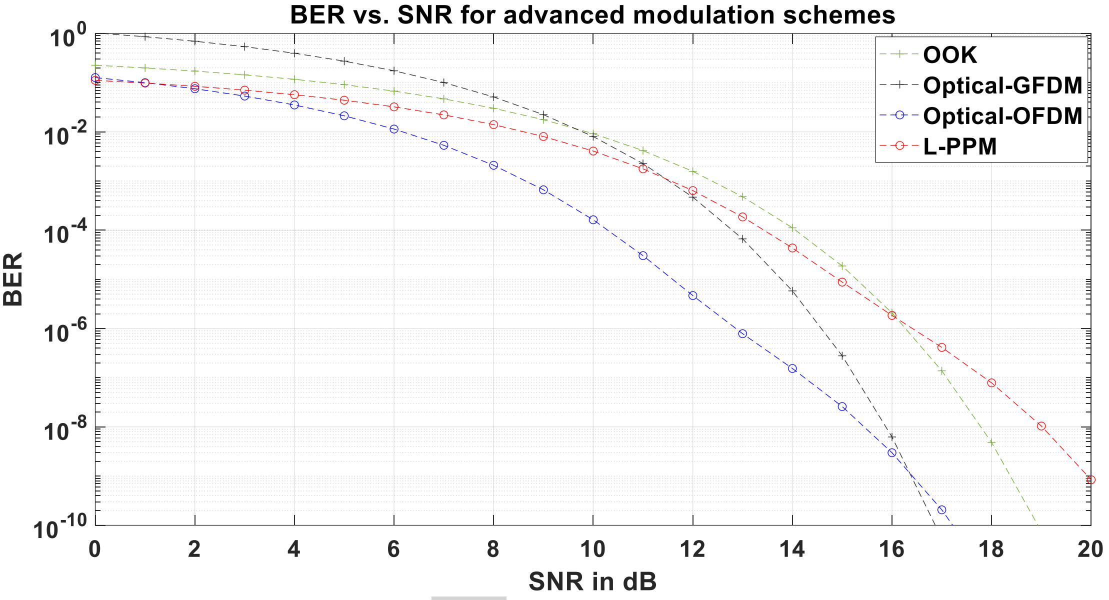

Fig. 2 BER vs. SNR.

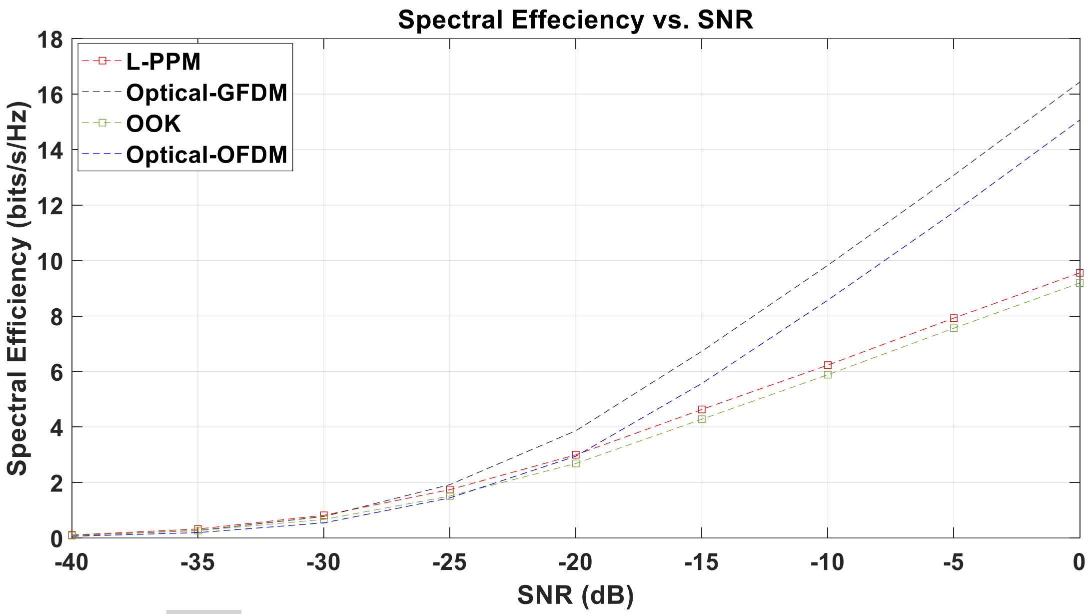

Fig. 3 Spectral Efficiency vs. SNR with Beamforming Function.

4.CONCLUSIONS

To enhance system performance and guarantee power and bandwidth efficiency, advanced modulation techniques-based beamforming functions for OWC were developed in this study. Particularly, the beamforming function with multiple sources at the transmitter and multiple apertures at the receiver has been considered when deriving the mathematical models of several modulation methods for the proposed system (L-PPM, optical-OFDM, and optical-GFDM). According to the findings of this investigation, the optical-GFDM assisted beamforming function performs better in terms of bandwidth efficiency and power efficiency than the other study-involved methods. One of the significant conclusions from this work is that, at the expense of adding complexity, the beamforming function improves the spectral efficiency for various methods.

ACKNOWLEDGEMENTS

The authors are grateful for the financial support for this research by the Information and Communication Engineering Department, Al-Khwarizmi College of Engineering, University of Baghdad. The research project was registered by the Information and Communication Engineering Department Council No. 2 /Sep. 2022.

REFERENCES

[1] Paramjot S, Harmandar K. **Analysis of FSO Based ROF-WDM System with Advance Intensity Modulation Techniques under Various Atmospheric Conditions**. *2nd International Conference on Electronics, Communication and Aerospace*

Technology (ICECA)* 29-31 March 2018; Coimbatore, India: p. 445-449.

[2] Nawaf SF. **Channel Capacity Improvement of MIMO Communication Systems using Different Techniques**. *Tikrit Journal of Engineering Sciences* 2018; **25** (1): 36–41.

[3] Noor K, Walid A, Falah H, Israa M. **Efficient Resource Allocation for Wireless-Powered MIMO-NOMA Communications**. *IEEE Access* 2022; **10**: 130302-130313.

[4] Maha M, Saad M, Asmaa S. **A New Transmission and Reception Algorithms for Improving the Performance of SISO/MIMO- OFDM Wireless Communication System**. *Tikrit Journal of Engineering Sciences* 2021; **28** (3): 146–158.

[5] Esam M, Mohammed T. **Error Analysis of NOMA-Based VLC Systems with Higher Order Modulation Schemes**. *IEEE Access* 2020; **8**: 2792-2803.

[6] Samir A, Mohd F, Ali A, Redhwan Q, Usman U, Nasir A, Tarik A. **A Survey of Free Space Optics (FSO) Communication Systems, Links, and Networks**. *IEEE Access* 2020; **9**: 7535-7373.

[7] Layla M, Thuraya M, Jalal J. **Performance Analysis of Different Flexible Decoding Algorithms for NR-LDPC Codes: Performance Analysis**. *Tikrit Journal of Engineering Sciences* 2022; **29** (4): 10–18.

[8] Yue Y, Miao L, Guan G, Hikmet S. **Resource Allocation for UAV-Assisted MIMO-NOMA Wireless Caching Networks**. *IEEE 21st International Conference on Software Quality, Reliability and Security Companion (QRS-C)* 2021; Hainan, China: p. 1006-1010.

[9] Erik G, Edfors O, Fredrik T, Thomas L. **Massive MIMO for Next Generation Wireless Systems**. *IEEE Communications Magazine* 2014; **52** (2):186-195.

[10] Ahmed T, Mohammad T, Ahmed H, Hasanain N, Ali M, Farah A. **Performance Evaluation of Wireless Data Traffic in Mm Wave Massive MIMO Communication**. *Indonesian Journal of Electrical Engineering and Computer Science* 2020; **20** (3): 1342-1350.

[11] Gassemlooy Z, Popoola W, Rajbhandari S. **Optical Wireless Communications: System and Channel Modelling with MATLAB.** 2nd ed., Florida, USA: CRC Press, Taylor & Francis Group; 2018.

[12] Israa H, Ayad A. **Energy-Efficient Massive MIMO Network**. *Tikrit Journal of Engineering Sciences* 2023; **30** (3):1-8.

[13] Muhammad S, Gucluoglu T. **Maximum Ratio Transmission Based Generalized Frequency Division Multiplexing Over Gamma-Gamma Channel**. *Optical Communications* 2021; **492**: 1-8.

[14] Wilson S, Brandt-Pearce M, Qianling C, Leveque J. **Free-Space Optical MIMO Transmission with Q-ary PPM**. *IEEE Transactions on Communications* 2005; **53** (8): 1402–1412.

[15] Björnson E, Hoydis J, Sanguinetti L. **Massive MIMO Networks: Spectral, Energy, and Hardware Efficiency**. 1st ed., Now Foundations and Trends; 2017.

[16] Wan J, Hongzhan L, Jianjun Y, Zhongchao W, Aiping L, Dongmei D. **Performance of a QAM/FSO Communication System Employing Spatial Diversity in Weak and Saturation Turbulence Channels**. *Journal of Modern Optics* 2019; **66** (9): 965–975.

[17] Al-Nahhal M, Tawfik I. **Enhancing Spectral Efficiency of FSO System Using Adaptive SIM/M-PSK and SIMO in the Presence of Atmospheric Turbulence and Pointing Errors**. *International Journal of Communication Systems* 2019; **32** (9): 1-12.

[18] Anshul J, Manav R, Virander K. **Performance Evaluation of Space Shift Keying in Free-Space Optical Communication**. *Journal of Optical Communications and Networking* 2017; **9** (2):149–160.

[19] Seung-Hoon H, Yan C. **SIM/SM-Aided Free-Space Optical Communication with Receiver Diversity**. *Journal of Lightwave Technology 2014*; **32** (14):2443–2450.

[20] Kehinde O, Pius A, Viranjay M. **Performance Analysis of Free Space Optical System with Spatial Modulation and Diversity Combiners Over the Gamma Gamma Atmospheric Turbulence**. *Optics Communications 2017*; **382**:205–211.

[21] Hien T, Ngoc T. **Performance Improvement of Spatial Modulation-Assisted FSO Systems over Gamma–Gamma Fading Channels with Geometric Spreading**. *Photonic Network Communications 2017*; **34** (2): 213–220.

[22] Chien-Chun C, Hikmet S, Serdar S, Yu T. **Enhanced Spatial Modulation with Multiple Signal Constellations**. *IEEE*

Transactions on Communications 2015; **63** (6): 2237–2248.

[23] Lwaa F, Sripati U, Muralidhar K. **BER Performance Improvement of Dual Chaotic Maps Based on STBC Communication System**. *Al-Khwarizmi Engineering Journal* 2022; **18** (4):32-44.

[24] Lwaa F, Tabarek A. **Performance Analysis for Hybrid Massive MIMO FSO/RF Links Based on Efficient Channel Codes**. *International Journal of Intelligent Engineering and Systems 2021*; **6** (14):333-343.